

Supplementary Information

The potential of zwitterionic nanoliposomes against neurotoxic alpha-synuclein aggregates in Parkinson's Disease

Farhang Aliakbari ^{1,2,3}, Hossein Mohammad-Beigi ^{1,2,4}, Nasrollah Rezaei-Ghaleh ⁵, Stefan Becker ⁶, Faezeh Dehghani Esmatabad ¹, Hadiieh Alsadat Eslampanah Seyedi ^{1,7}, Hassan Bardania ⁸, Amir Tayaranian Marvian ^{1,9}, Joanna F. Collingwood ¹⁰, Gunna Christiansen ¹¹, Markus Zweckstetter ^{5,6,12}, Daniel E. Otzen ^{* 2} and Dina Morshedi ^{*1}

1. Bioprocess Engineering Department, Institute of Industrial and Environmental Biotechnology, National Institute of Genetic Engineering and Biotechnology, Tehran, Iran.
2. Interdisciplinary Nanoscience Centre (iNANO) and Department of Molecular Biology and Genetics, Aarhus University, Gustav Wieds Vej 14, DK-8000 Aarhus C, Denmark.
3. Department & Center for Biotechnology Research, School of Medicine, Semnan University of Medical Sciences, Semnan, Iran.
4. Biotechnology Group, Faculty of Chemical Engineering, Tarbiat Modares University, P.O. Box 14115-143, Tehran, Iran.
5. Department of Neurology, University Medical Center Göttingen, Germany.
6. Department for NMR-based Structural Biology, Max Planck Institute for Biophysical Chemistry, Göttingen, Germany.
7. Institute for Glycomics, Griffith University, QLD, Australia.
8. Cellular and Molecular Research Center, Yasuj University of Medical Sciences, Yasuj, Iran.
9. Department of Translational Neurodegeneration, German Center for Neurodegenerative Diseases (DZNE), D-81377, Munich, Germany.
10. School of Engineering, University of Warwick, Coventry, UK.
11. Department of Biomedicine, Aarhus University, 8000 Aarhus C, Denmark.
12. German Center for Neurodegenerative Diseases (DZNE), Göttingen, Germany.

* Corresponding Authors:

morshedi@nigeb.ac.ir (Morshedi. D.), National Institute of Genetic Engineering and Biotechnology, Address: Shahrak-e Pajooheh, km 15 Tehran - Karaj Highway, Tehran, Iran, P.O.Box:14965/161, Tehran, Iran, Tel: +9821-44878423, Fax: +9821-44878395

dao@inano.au.dk (Otzen. D. E.), Interdisciplinary Nanoscience Centre (iNANO) and Department of Molecular Biology and Genetics, Aarhus University, Gustav Wieds Vej 14, building 1592, 224.8000 Aarhus C, Denmark. Mobile: +4520725238

Experimental procedures

α SN preparation

pNIC28-Bsa4 plasmid containing the human α SN cDNA was transformed to the *Escherichia coli* BL21 (DE3) pLysS cells and 0.5 mM IPTG was used to induce gene expression at OD₆₀₀ between 0.6-0.8. α SN was extracted and then purified by three steps including osmotic shock, anion-exchange chromatography and size exclusion chromatography¹. The protein was freeze-dried and stored at -20°C prior to use.

In order to label α SN, fluorescein isothiocyanate (FITC) which is a fluorescent probe and is conjugated with lysine residues, was used. FITC (1 mg/ml in DMSO) at a ratio of 1:10 (W/W) was added to α SN (1 mg/ml in PBS) and incubated at 37°C for 30 min. The labeled protein was used to assess the possible interaction of α SN with NLP-Chol and NLP-Chol-PEG.

Seed preparation and the secondary nucleation assays

In order to evaluate the influence of NLPs on the lag or log phases of α SN fibrillization, the fibril elongation assays were accomplished using the same procedure as for the fibril formation assay in which the seeds composed of pre-formed fibrils of α SN were added to α SN with or without NLPs at the beginning of the fibrillization process^{1,2}. For this purpose, the fibrils obtained from the plateau phase of fibrillization (equivalent to $70\ \mu\text{M}$ of monomer) were centrifuged for 30 min at 13000 rpm, and then the supernatant was decanted and the pellet was re-suspended in the same buffer use for α SN fibrillization. To acquire seeds, the sample was then sonicated for 5 min in a water bath sonicator with the power of 5 % (BANDELIN SONOREX Digital 10 P sonicator, Germany). Thereafter, a 5% (v/v) of the seeds were added to monomer of α SN ($70\ \mu\text{M}$)

supplemented by either NLP-Chol or NLP-Chol-PEG (280 μM) and incubated at 37 $^{\circ}\text{C}$ with shaking at 80 rpm and the kinetics of fibrillization were then measured.

Fibril disaggregation measurement

Either 280 μM of NLP-Chol or NLP-Chol-PEG were added to the end product of αSN (70 μM) fibrillization process and incubated at 37 $^{\circ}\text{C}$ either without or with shaking (300 rpm) in a 96-well-plate containing glass beads. To remove any possible monomers available in the end-product of αSN , the materials were first centrifuged at 13000 rpm for 30 min and then the pellet was dissolved in PBS and used as mature fibrils for disaggregation.

ThT fluorescence intensity measurement

ThT fluorescence intensity was used to monitor the kinetic of αSN fibrillization. For this purpose, a sample of 20 μl of incubated αSN solution in the presence or absence of NLPs was added to 480 μl of 12 μM ThT, an amyloid-specific fluorophore, which was dissolved in 10 mM Tris (pH 8.0). The excitation and emission slit widths were adjusted to 5 and 10 nm respectively. The fluorescence spectra were then taken in the emission range of 450-550 nm with excitation at 440 nm using a Cary Eclipse VARIAN fluorescence spectrophotometer (Mulgrave, Australia).

Atomic Force Microscopy (AFM)

Samples of αSN (70 μM) fibrillated in the presence or absence of NLPs were diluted 20 times in filtered deionized water. An aliquot of 10 μl was spread on freshly cleaved mica sheets, dried, and washed twice with de-ionized water. AFM was performed on a Veeco (Veeco Instruments Inc. USA, NY) with a silicon probe (CP). Imaging was performed in noncontact mode.

Transmission Electron Microscopy (TEM)

5 μ L samples were deposited on a carbon-coated, glow-discharged 400-mesh grid for 30 s. Then the grids were rinsed with two droplets of double distilled water, and stained with 1% phosphotungstic acid (pH 6.8), and then blotted dry. The samples were analyzed by electron microscopy (JEM-1010; JEOL, Tokyo, Japan) at 60 kV and the images were taken using an Olympus KeenView G2 camera.

Circular dichroism (CD) analysis

CD spectra were acquired in the far-UV region at 190–260 nm at room temperature employing 100 μ g/mL of protein on an AVIV 215 spectropolarimeter (Aviv Associates, Lakewood, N.J., U.S.A.), in 0.1-cm circular cuvettes. Appropriate background spectra were subtracted to obtain signals from α SN and data were converted to mean residue molar ellipticity (MRE).

Sodium dodecyl sulphate-Polyacryl amid gel electrophoresis (SDS-PAGE) analysis to detect the interaction of α SN with NLPs

SDS-PAGE was employed to observe the aggregated species of α SN which may interact with NLPs. The samples including α SN incubated alone or in the presence of NLPs were centrifuged for 10 min at 5000 rpm to isolate the NLPs and precipitate NLPs which had interacted with α SN. The pellets were dissolved first in PBS and then in sample buffer. The supernatants were divided in two fractions. One fraction was precipitated using 10% trichloroacetic acid (TCA) and then dissolved in sample buffer. The second fraction was centrifuged again at 13000 rpm for 30 min to pellet the fibrils and the pellets were then dissolved in sample buffer. All samples were run on a 12% gel.

1,2-Dimyristoyl-*sn*-glycero-3-phosphorylglycerol sodium salt (DMPG) SUV preparation

5 mg/mL DMPG was dissolved in 1 mL PBS and then subjected to 10 cycles of freeze-thaw in liquid nitrogen and being raised to 50 °C. The material was then extruded 21 times through a 100 nm filter.

NLPs free radical scavenging activity

The potential of NLP-Chol and NLP-Chol-PEG to scavenge free radicals was assessed by vanishing the DPPH• from medium. 200 µL of DPPH• solution (100 µM dissolved in methanol) was added to 100 µL of different concentrations of either NLP-Chol or NLP-Chol-PEG (35, 70, 140, 280, 560 µM) and incubated for 30 min in the dark at room temperature. The calorimetric experiment was then performed at 517 nm.

αSN-overexpressing SHSY5Y cell generation

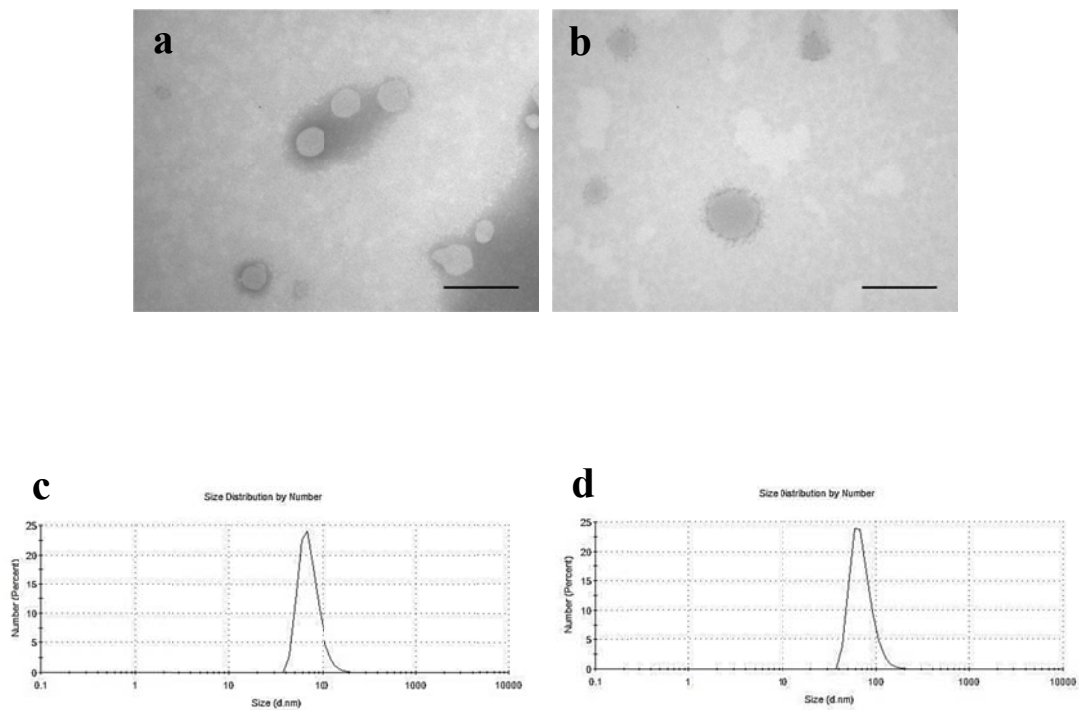
A lentiviral infection method³⁻⁵ was employed to infect the SHSY5Y cells with a lentiviral vector containing the αSN gene. Accordingly, the αSN gene complemented with digestion sites of NotI (5' GCGGCCGC 3') and MluI (5' ACGCGT 3') and a Kozak sequence (5' ccaccatgg 3') was synthesized and cloned into the pLEX-JRed-TurboGFP lentiviral plasmid which contains the kanamycin and puromycin resistance genes for selection in bacteria and stable transductant respectively (the plasmid was a gift from Stem Cell Technology Research Center, Tehran, Iran). The obtained construct along with packaging plasmid (p.MD2. G) and envelope plasmid (psPAX2) were transfected to the HEK293T cell line using the calcium phosphate method. The supernatant of the cell culture medium containing the viruses was collected 48 hours after the transfection and concentrated using PEG6000. To determine the viral titer, HEK293T cells were infected with concentrated viruses. For this purpose, a total of 120,000 cells/well were cultured into the 24-well plate and 5 fold serial dilutions (1:5, 1: 25; 1:125; and 1:625) of concentrated

viruses were prepared and then 10 μL of each were added to an individual well. To determine the reporter positive cells, flow cytometry was performed after 48 hours of incubation and the viral titer was calculated using the following equation:

$$\textit{Titer} = \frac{\text{Cell number} \times \% \text{ of positive reporter cells} \times \text{dillution factor}}{\textit{Vector volume (ml)} \times 100}$$

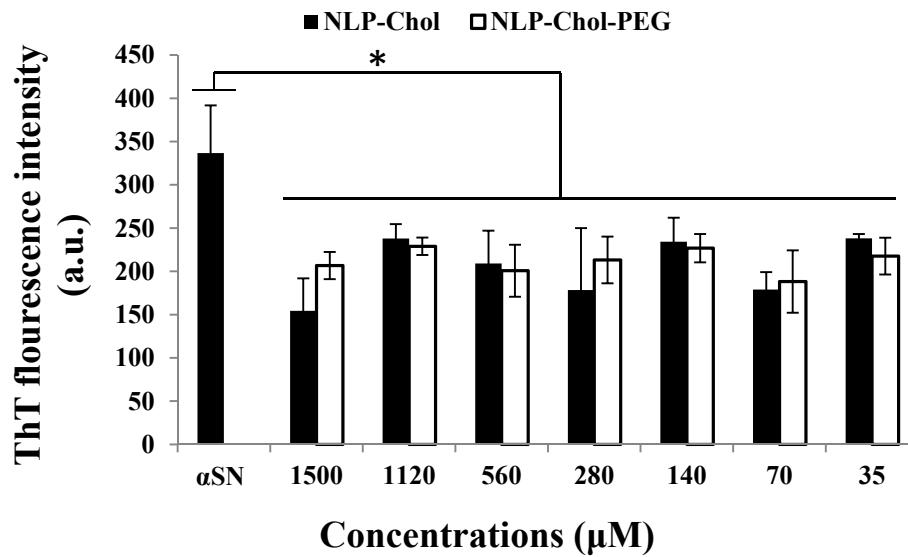
The SHSY5Y cells were then infected with appropriate MOI and the infected cells were selected using 0.2 $\mu\text{g}/\text{mL}$ puromycin.

Supplementary Figure. 1.



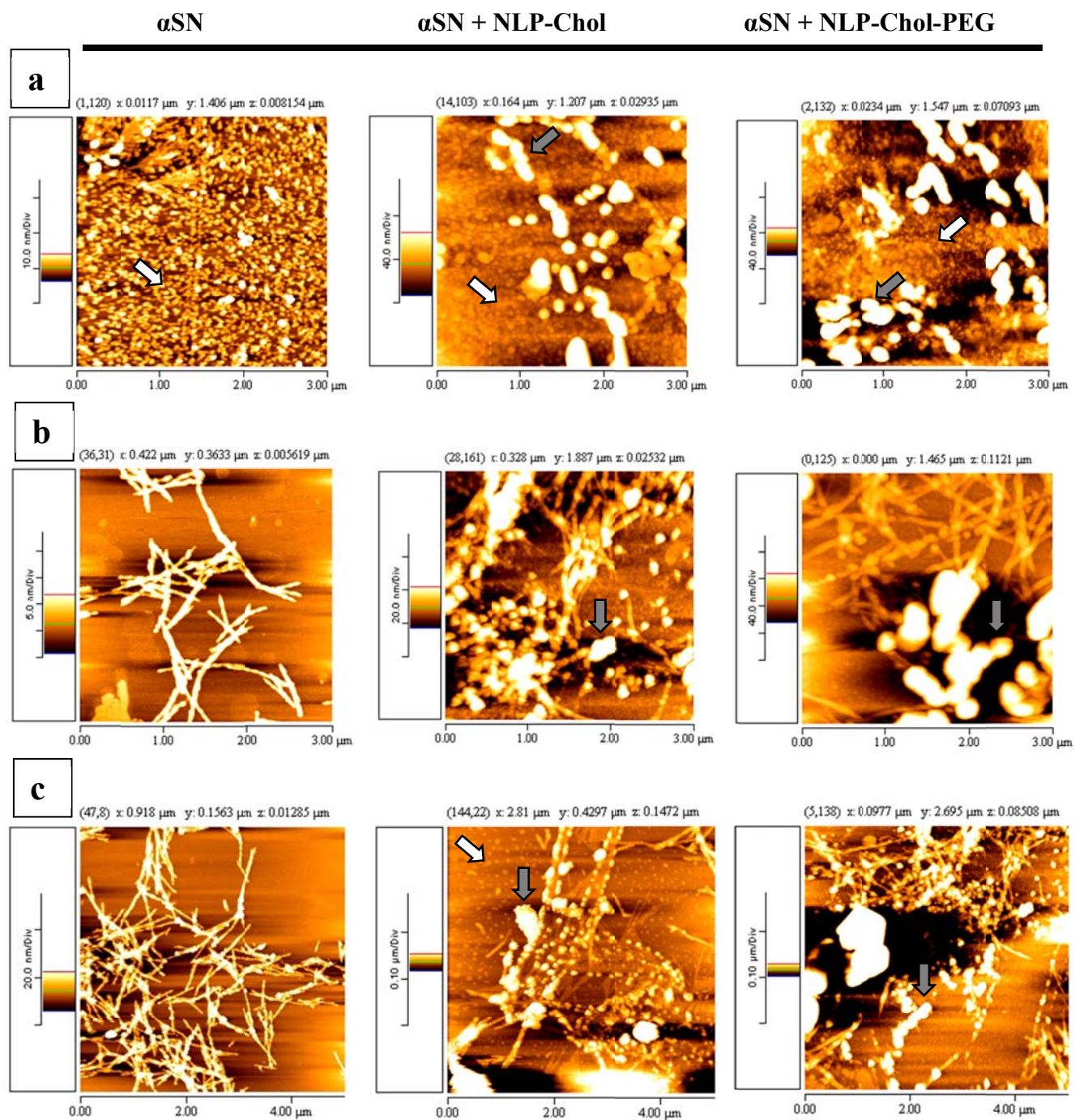
Supplementary Figure. 1. The morphology and size of NLPs. Transmission electron microscopy images of NLP-Chol (a) and NLP-Chol-PEG (b). Scale bar, 200 nm. Size distribution by number for NLP-Chol (c) and NLP-Chol-PEG (d) measured by dynamic light scattering.

Supplementary Figure. 2.



Supplementary Figure. 2. αSN fibril formation in the absence or the presence of different concentrations of NLP-Chol and NLP-Chol-PEG using ThT fluorescence intensity after 24 hours of incubation. Results from αSN incubated with different concentrations of NLPs are significantly dissimilar from those of controls (αSN incubated alone) (mean \pm SD, $n=3$, $*p \leq 0.05$).

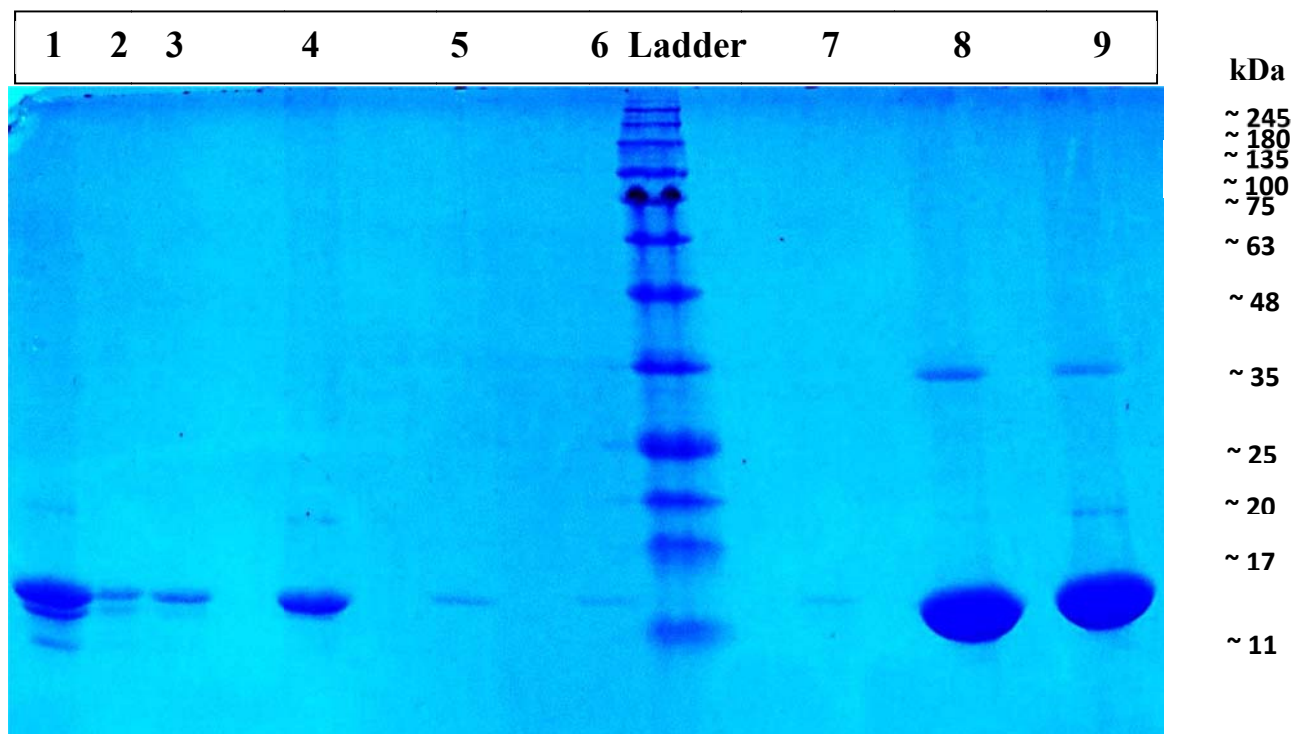
Supplementary Figure. 3.



Supplementary Figure. 3. AFM images for the α SN incubated over 28 hours in the presence or absence of NLP-Chol and NLP-Chol-PEG. The images show the amount and shape of oligomers

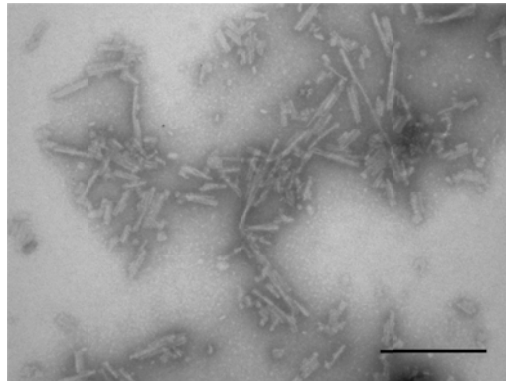
and fibrils at three time points. The morphology of fibrils are almost the same in all treated and untreated samples and have a twisted structure which indicates a common fibrillization pathway in all the samples. α SN incubated in the presence of NLPs appears to retain its oligomeric form even after 18 hours of incubation, whilst in the absence of NLPs the fibrillar form of the protein was observed after 7 hours of incubation. The free monomers and oligomers in treated samples start to fibrillize with a delay compared to untreated samples but via the same fibrillization pathway. The images represent α SN incubation at 8 hours (a), 18 hours (b), and 28 hours (c) in the absence (left) or presence of NLP-Chol (middle) and NLP-Chol-PEG (right). The white arrows indicate oligomers, the grey arrows indicate NLPs.

Supplementary Figure. 4.



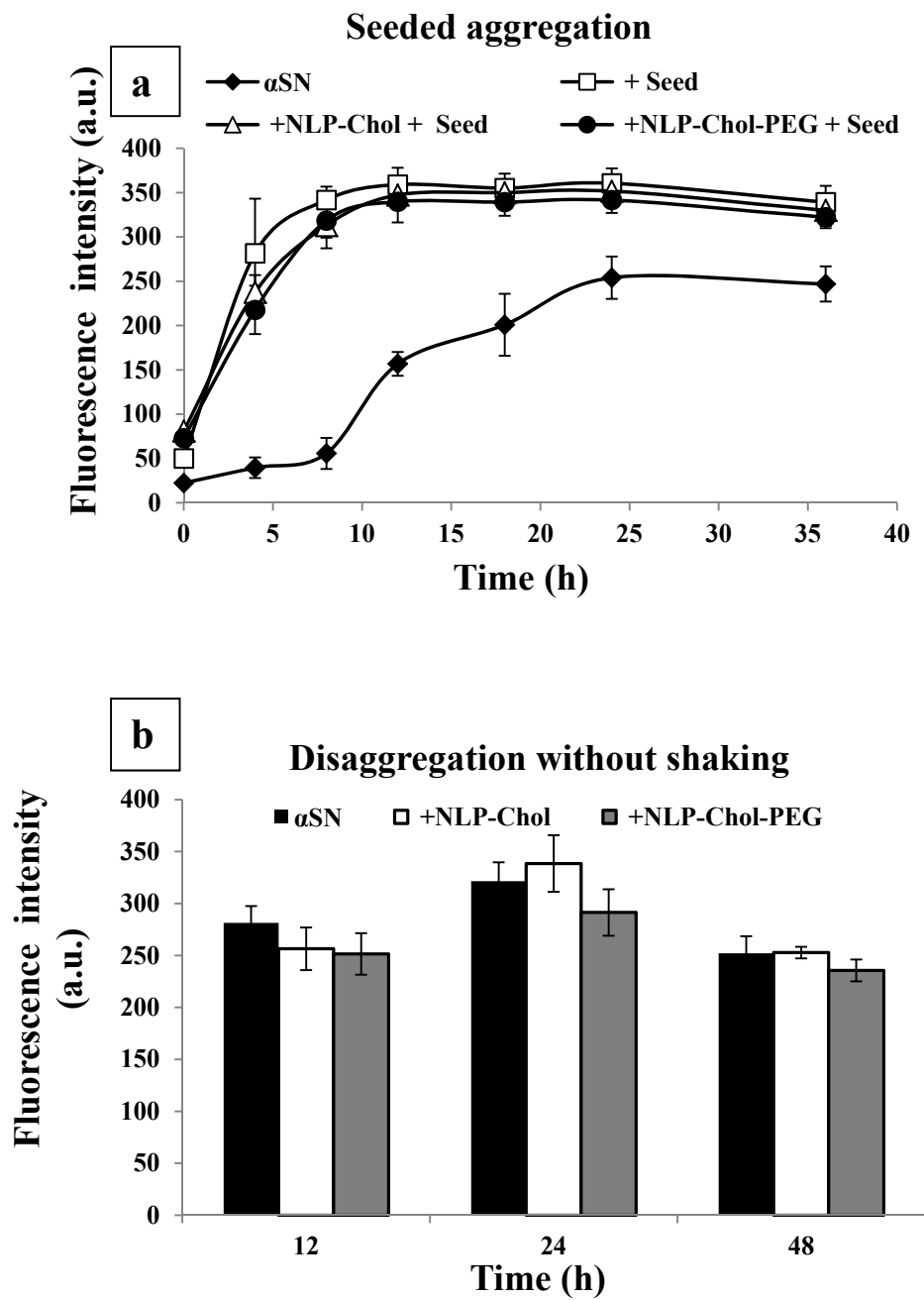
Supplementary Figure. 4. SDS-PAGE analysis of α SN incubated in the absence or presence of NLPs loaded on a 12% gel after 48 hours of incubation. The final products were centrifuged for 10 min at 5000 rpm to precipitate the NLPs and the supernatants were divided into two parts. One part was precipitated with 10% Trichloroacetic acid (TCA), dissolved in sample buffer and loaded onto the gel (1-3; 1: α SN alone, 2: α SN in the presence of NLP-Chol and 3: α SN in the presence of NLP-Chol-PEG). The second part was further centrifuged at 13000 rpm for 30 min to precipitate the fibrils and the pellets were dissolved in sample buffer and loaded onto the gel (4-6; 4: α SN alone, 5: α SN in the presence of NLP-Chol and 6: α SN in the presence of NLP-Chol-PEG). The pellets from the first centrifugation step (10 min at 5000 rpm) were also loaded onto the gel (7-9; 7: α SN alone, 8: α SN in the presence of NLP-Chol and 9: α SN in the presence of NLP-Chol-PEG).

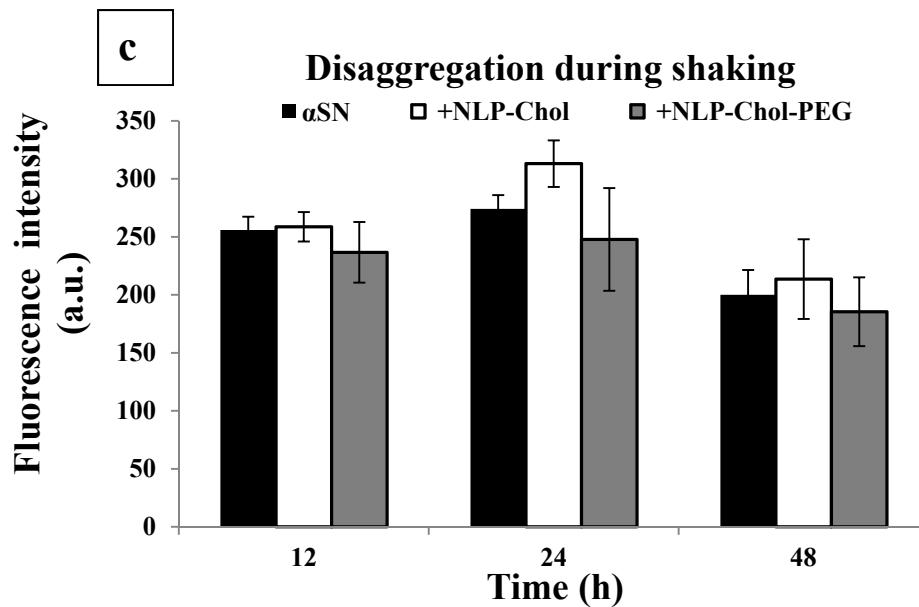
Supplementary Figure. 5.



Supplementary Figure. 5. TEM image shows the morphology of seeds to determine the secondary pathway of α SN fibrillization. α SN was dissolved in PBS and incubated at 37 °C. To assess the effect of NLPs on the secondary nucleation as an important pathway responsible for the production of fibrils, the pre-formed fibrils derived from the plateau phase of fibrillization were sonicated and used as seeds to eliminate the primary nucleation phase.

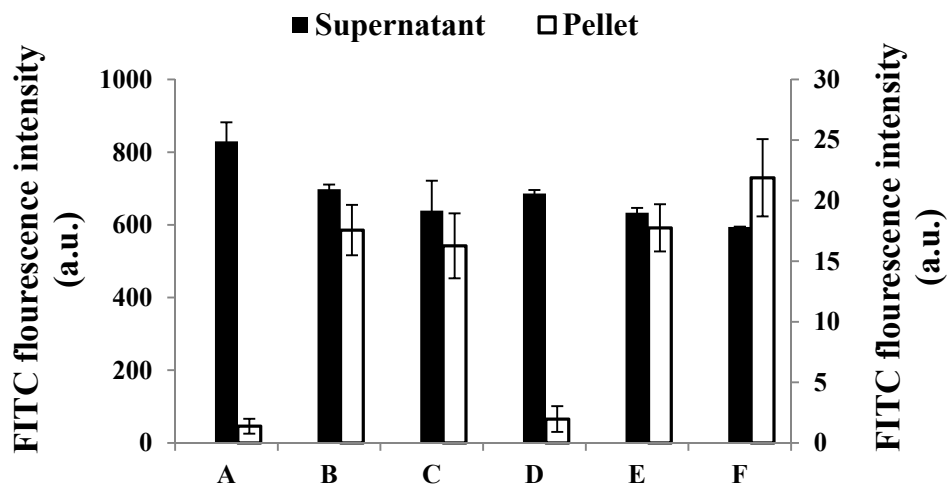
Supplementary Figure. 6.





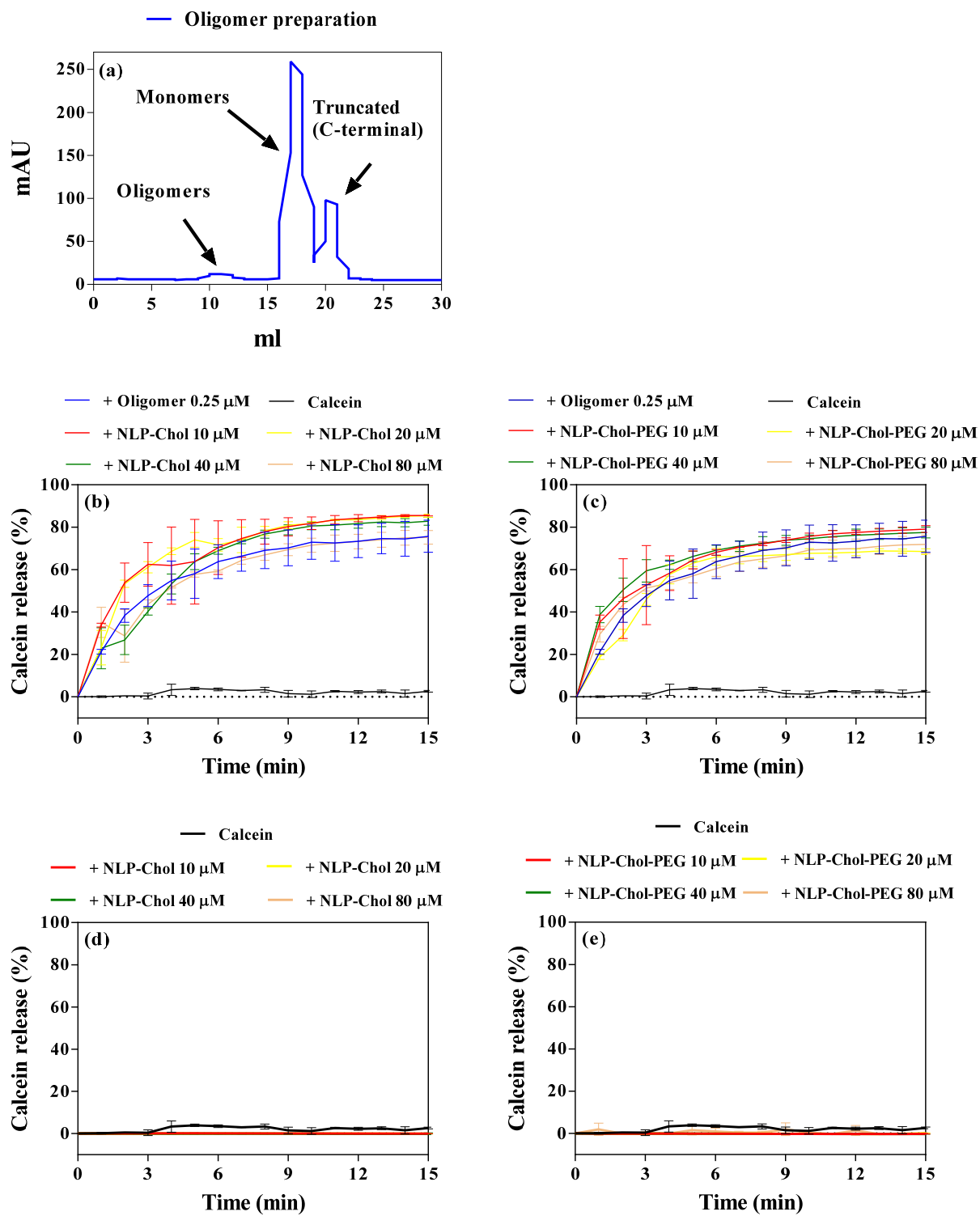
Supplementary Figure. 6. The effect of the NLP-Chol and NLP-Chol-PEG on the seeding of α SN fibrillization and disaggregation. (a) ThT results of the aggregation of α SN (70 μ M), alone or supplemented by NLP-Chol or NLP-Chol-PEG (280 μ M) seeded by 5% of mature sonicated fibrils. (b) Disaggregation of α SN fibrils in the absence or presence of NLP-Chol or NLP-Chol-PEG (280 μ M) with no shaking or (c) while being shaken (300 rpm). No significant differences were observed. The excitation and emission for ThT were 440 and 480 nm respectively.

Supplementary Figure. 7.



Supplementary Figure. 7. Assessing the interaction of α SN with NLPs by measuring the protein in the supernatant and pellet of α SN incubated with or without NLPs using FITC fluorescent. A: monomer of α SN, B: monomer + NLP-Chol, C; monomer + NLP-Chol-PEG, D: short-term incubated (2-3 hours of incubation) α SN, E: short-term incubated α SN + NLP-Chol, F: short-term incubated α SN + NLP-Chol-PEG.

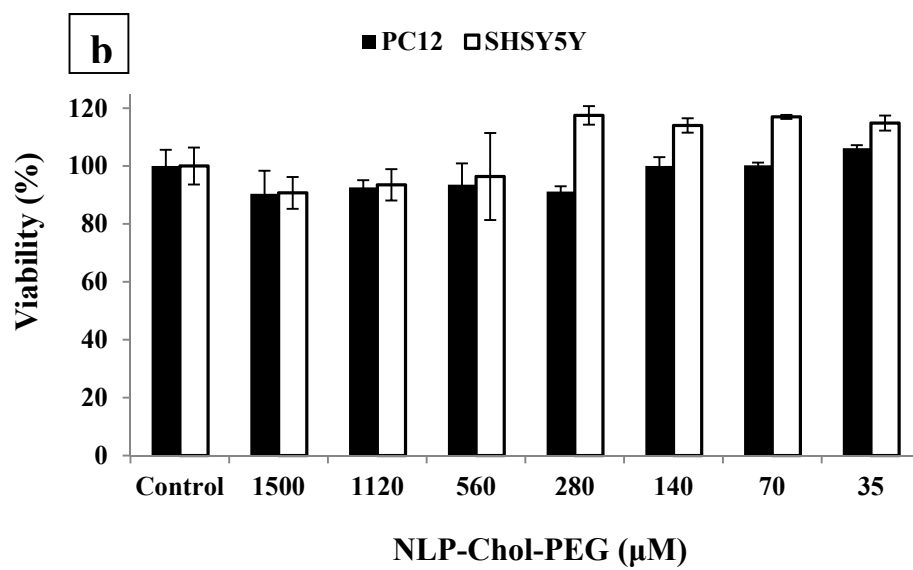
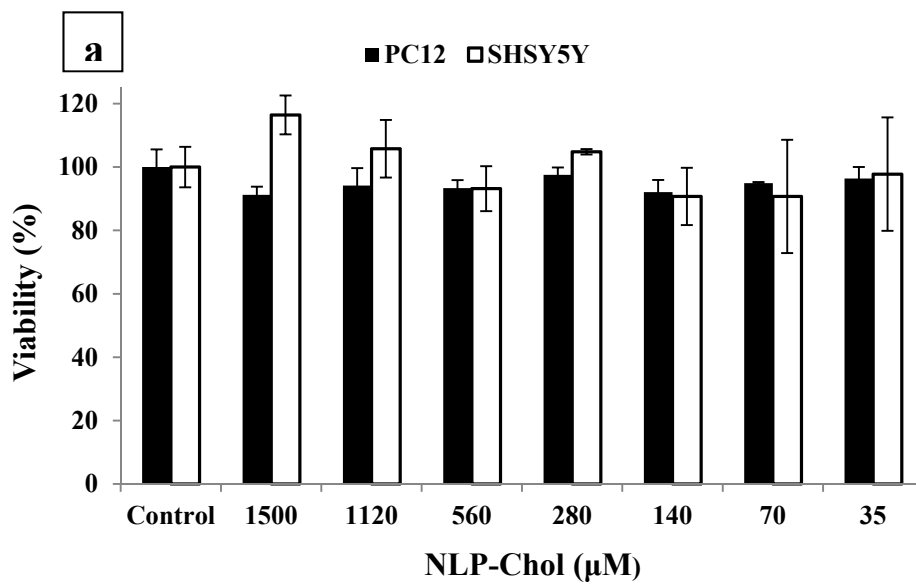
Supplementary Figure 8.

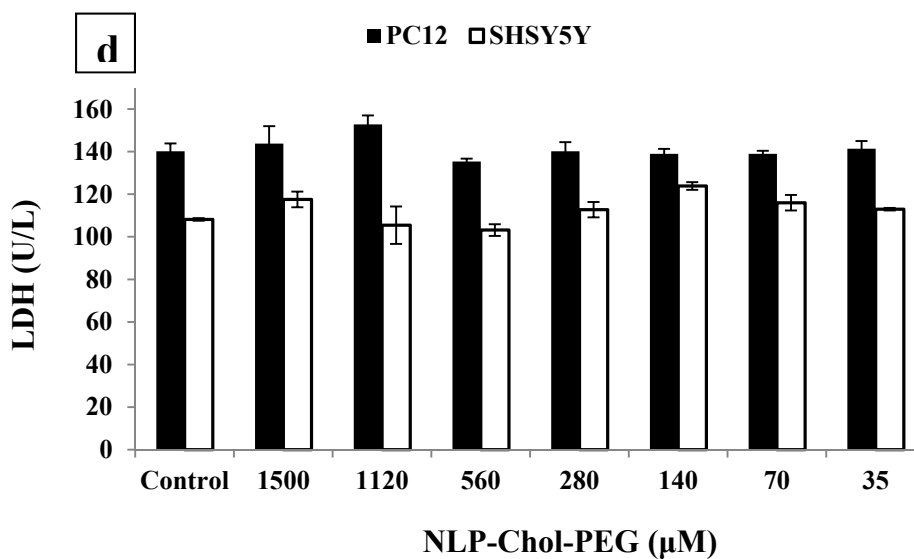
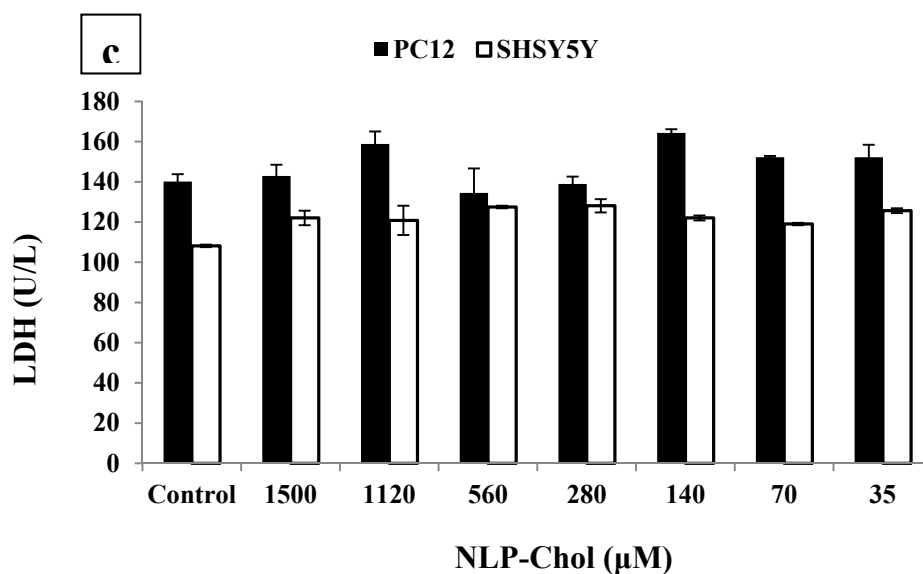


Supplementary Figure 8. Oligomer preparation (a) and calcein release from DOPG vesicles (b-

e). Calcein release was assessed while DOPG vesicles were treated with oligomers in the presence of NLP-Chol and NLP-Chol-PEG (b and c) or just NLPs alone (d and e).

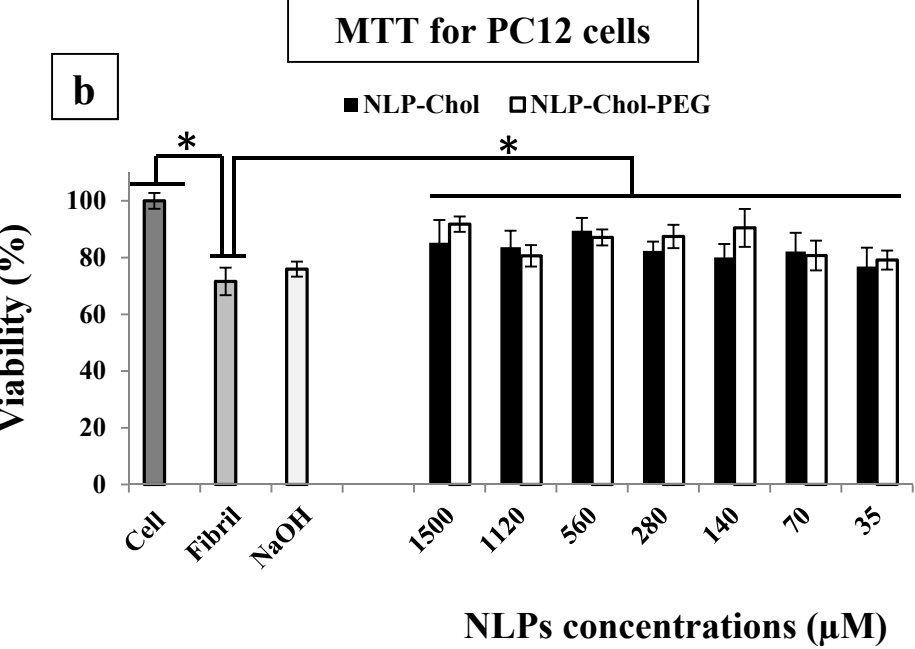
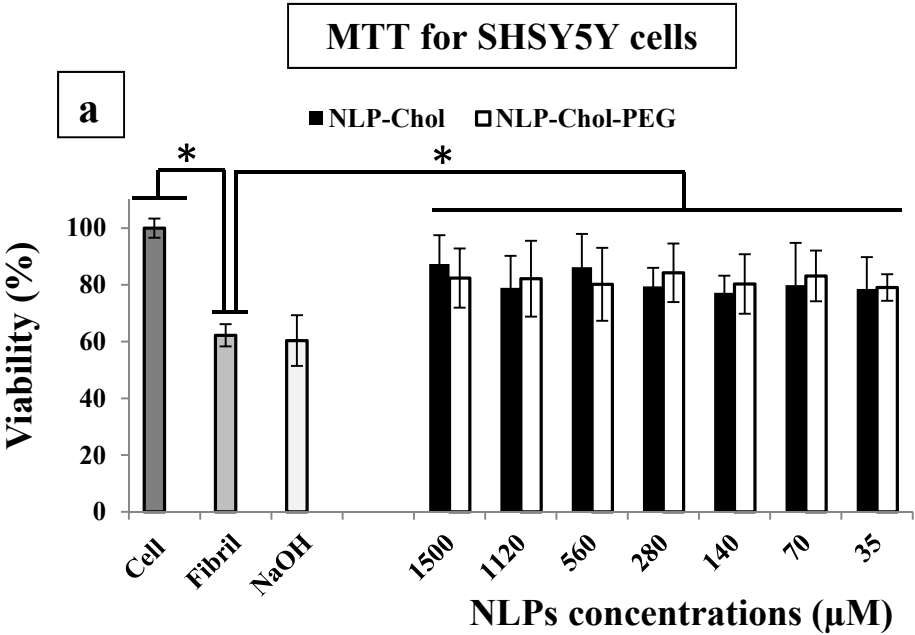
Supplementary Figure. 9.

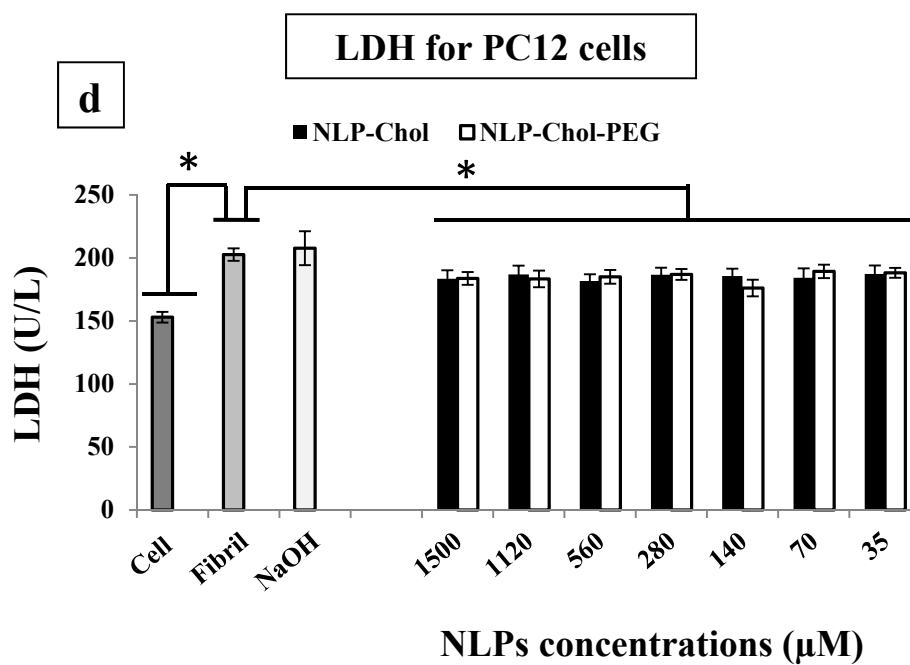
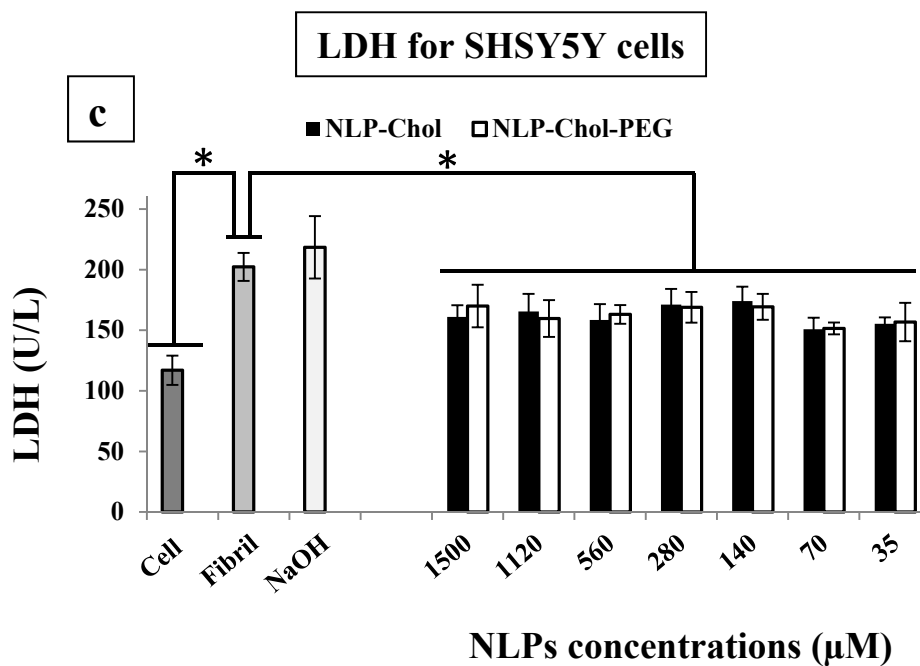




Supplementary Figure. 9. Neurotoxicity of different concentrations of NLPs on the PC12 and SHSY5Y cell lines after 24 hours of incubation using MTT and LDH assays. (a) The percentage of cell viability treated with NLP-Chol using MTT assay. (b) The percentage of cell viability treated with NLP-Chol-PEG using MTT assay. (c) The amount of released lactate dehydrogenase from the cells treated with NLP-Chol. (d) The amount of released lactate dehydrogenase from the cells treated with NLP-Chol-PEG.

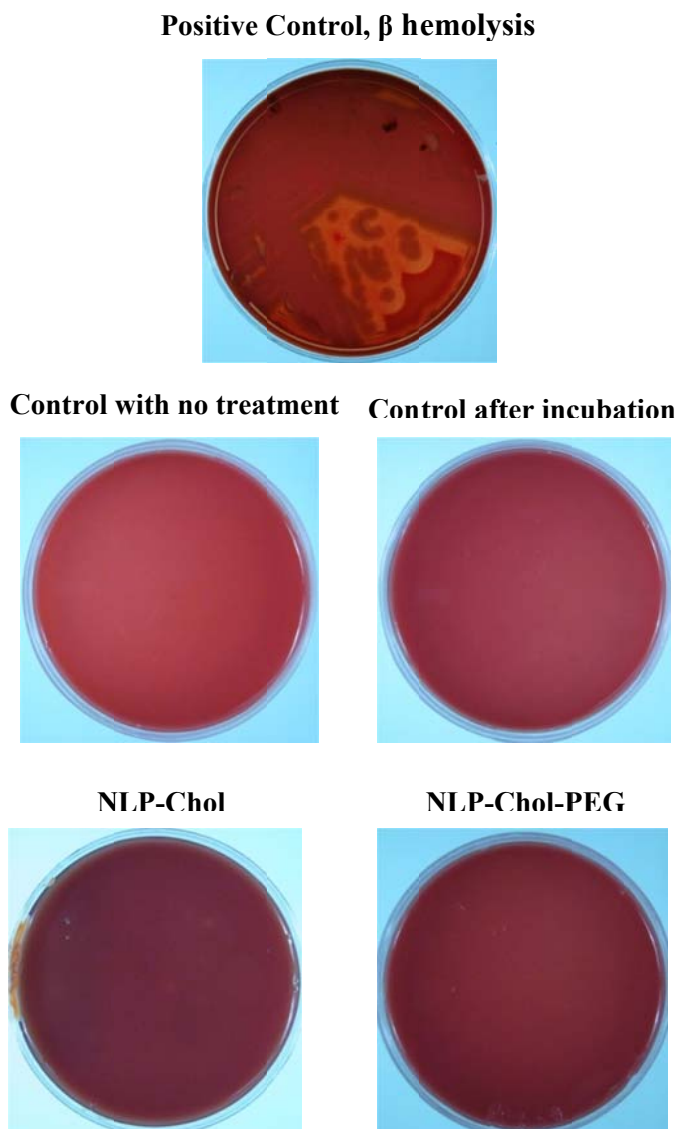
Supplementary Figure. 10.





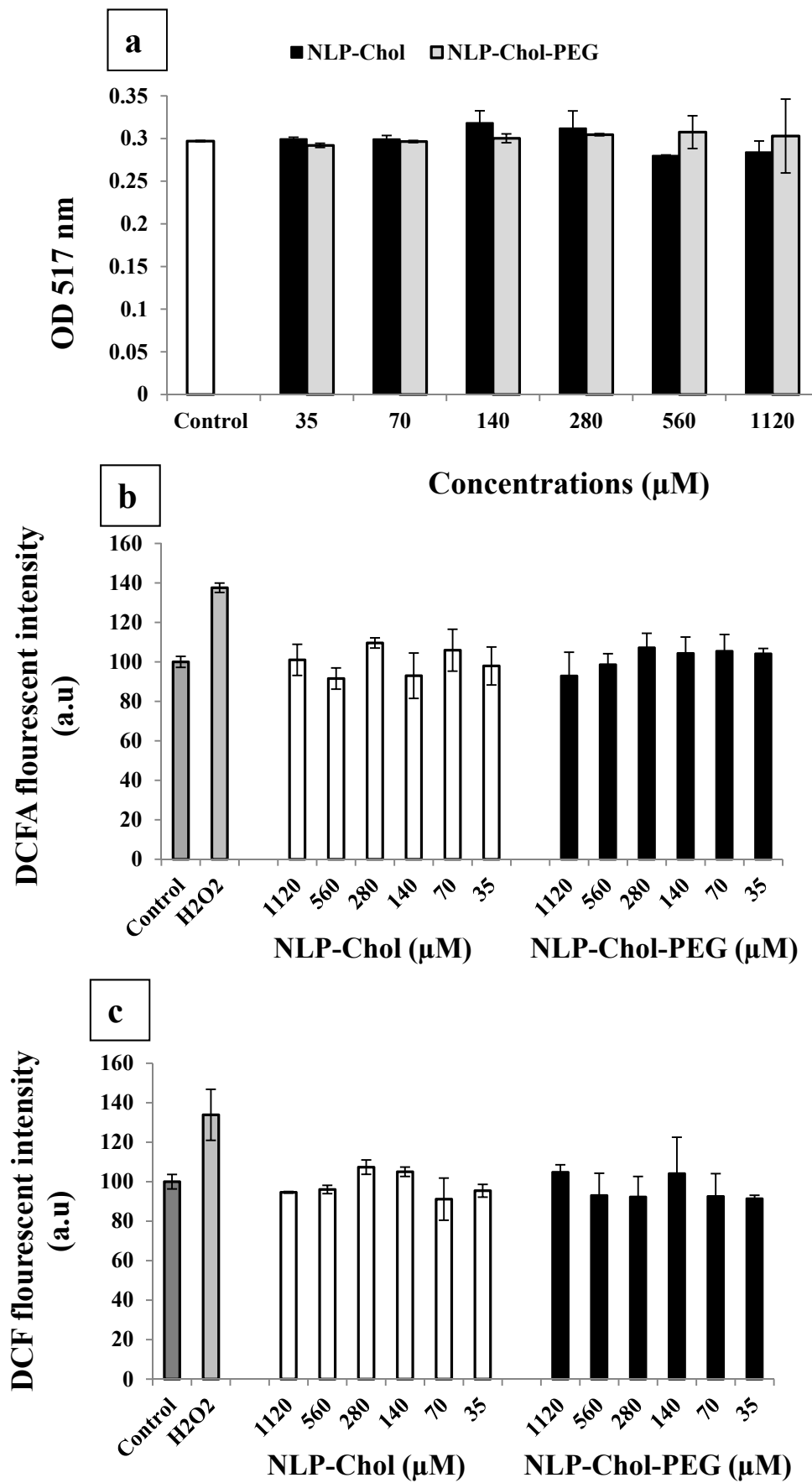
Supplementary Figure. 10. Neurotoxicity assessment of α SN (70 μ M) in the presence or absence of different concentrations of NLP-Chol and NLP-Chol-PEG during the fibrillization process after 24 hours of incubation using MTT (a and b) and LDH (c and d) for SHSY5Y cells (a and c) and PC12 cells (b and d). Cytotoxicity percentages of α SN pre-incubated with NLPs were normalized to that of α SN pre-incubated alone and the outcome was statistically significantly different (* indicates $p \leq 0.05$).

Supplementary Figure. 11.



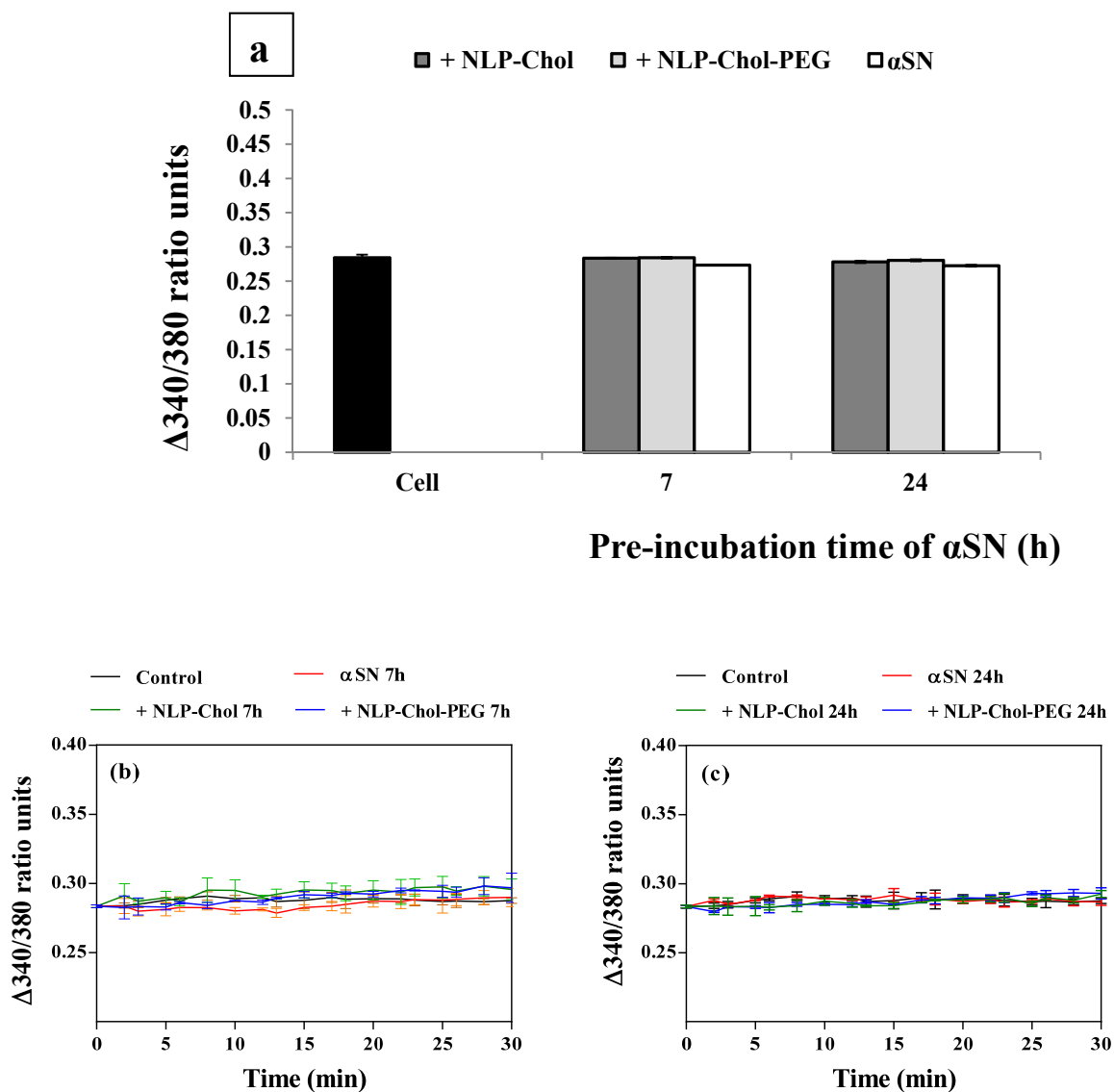
Supplementary Figure. 11. Hemolysis assay demonstrating biocompatibility of NLPs. A total of 100 μ L, NLP-Chol and NLP-Chol-PEG were spread onto the surface of blood agar medium (final concentration of 280 μ M). γ -hemolysis (no hemolysis) was perceived in the samples. β -hemolysis derived from *B. Cereus* was noticed in the control. γ -hemolysis was considered as biocompatibility of NLP-Chol and NLP-Chol-PEG.

Supplementary Figure. 12.



Supplementary Figure. 12. Free radicals scavenging activity of NLP-Chol and NLP-Chol-PEG based on DPPH assay (a). Assessment of the levels of ROS within the cells while being treated with different concentrations (35, 70, 140, 280, 560 and 1120 μM) of NLP-Chol and NLP-Chol-PEG after 6 hours of incubation for SHSY5Y cells (b) and PC12 cells (c). None of NLPs have the ability to scavenge radicals and did not show considerable antioxidant activity.

Supplementary Figure. 13.



Supplementary Figure. 13. The levels of intracellular calcium of SHSY5Y cells treated with α SN (70 μ M) pre-incubated alone or with NLP-Chol and NLP-Chol-PEG (280 μ M). α SN with or without NLPs was exposed to aggregating conditions and samples were taken after 7 hours and 24 hours. The cells were then treated with 7 h-aged and 24 h-aged aggregated species of α SN in the presence or absence of NLPs (a) and the intracellular calcium alteration was measured. The cells were also treated with the above materials and then immediately the amount of intracellular

calcium was measured for 30 min for 7 h-aged of α SN alone with or without NLP-Chol and NLP-Chol-PEG (b) and 24 h-aged of α SN alone with or without NLP-Chol and NLP-Chol-PEG (c).

References

- 1 D. Morshedi, F. Aliakbari, A. Tayaranian-Marvian, A. Fassihi, F. Pan-Montojo and H. Pérez-Sánchez, *J. Food Sci.*, 2015, **80**, H2336–H2345.
- 2 H. Mohammad-Beigi, S. A. Shojaosadati, A. T. Marvian, J. N. Pedersen, L. H. Klausen, G. Christiansen, J. S. Pedersen, M. Dong, D. Morshedi and D. E. Otzen, *Nanoscale*, 2015, **7**, 19627–19640.
- 3 M. Li, N. Husic, Y. Lin and B. J. Snider, *J. Vis. Exp.*, 2012, e4031.
- 4 D. Crabtree, M. Dodson, X. Ouyang, M. Boyer-Guittaut, Q. Liang, M. E. Ballestas, N. Fineberg and J. Zhang, *J. Neurochem.*, 2014, **128**, 950–961.
- 5 H.-J. Lee, E.-D. Cho, K. W. Lee, J.-H. Kim, S.-G. Cho and S.-J. Lee, *Exp. Mol. Med.*, 2013, **45**, e22.